Inhomogeneous strain in individual quantum dots probed by transport measurements

C. D. Akyüz[a)]
Department of Physics, Brown University, Providence, Rhode Island 02912

A. Zaslavsky and L. B. Freund
Division of Engineering, Brown University, Providence, Rhode Island 02912

D. A. Syphers
Physics Department, Bowdoin College, Brunswick, Maine 04011

T. O. Sedgwick
SiBond L. L. C., Hudson Valley Research Park, Hopewell Junction, New York 12533

(Received 8 December 1997; accepted for publication 7 February 1998)

Resonant tunneling measurements are used to probe the inhomogeneous strain in individual SiGe quantum dots. Current–voltage characteristics of strained Si/SiGe resonant tunneling diodes of diameter $D \leqslant 0.25$ μm exhibit additional fine quasi-periodic structure in the resonant peaks. The fine structure is consistent with lateral quantization in the SiGe quantum well due to in-plane confining potentials arising from inhomogeneous strain, which we calculate by finite element techniques for various D. Quenching of the fine structure by a magnetic field is consistent with the effective length scale of the strain-induced potential. © *1998 American Institute of Physics.* [S0003-6951(98)01514-9]

If a semiconductor heterostructure is lattice mismatched, the electronic properties are strongly influenced by the resulting strain. In a bulk mismatched heterostructure, the strain is biaxial and homogeneous, and its effects can be calculated explicitly.[1–3] Once a quantum wire or dot is fabricated, the in-plane homogeneity is lost and geometry-specific strain gradients appear. Previously, strain-induced confinement had been studied by photoluminescence measurements on large arrays of strained wires produced by stressor patterning[4] or epitaxial overgrowth.[5,6] Strain in quantum dots, which lack translational symmetry altogether, is even more complex and interesting.[7–9] We have probed the inhomogeneous strain in individual quantum dots of varying diameter D by a transport measurement. Our resonant tunneling data on strained $Si/Si_{1-x}Ge_x$ resonant tunneling (RT) diodes reveal a well-resolved fine structure arising from inhomogeneous strain-induced lateral quantization. The results are consistent with the confining potential predicted by finite element calculations. The predicted length scale of the confining potential is consistent with magnetic field-induced quenching of the fine structure.

Deep-submicron RT structures were fabricated from strained p-$Si/Si_{1-x}Ge_x$ double-barrier RT material. The details of the structural design were published previously[10,11]: the active regions consist of an $\sim$35 Å $Si/Si_{1-x}Ge_x$ quantum well confined by $\sim$45 Å Si barriers, sandwiched in turn by $Si/Si_{1-x}Ge_x$ emitter and collector reservoirs. Two designs with Ge content $x=0.25$ or 0.2 were employed. The processing involved the etching of a mesa of nominal diameter D followed by planarization and contact pad deposition.[11] A (SEM) micrograph of $D=0.15$ μm mesa prior to planarization is shown in Fig. 1. When a bias V is applied to the top contact, a tunneling current flows through the quantized hole subbands in the SiGe well, subject to the usual energy E and momentum $\mathbf{k}_\perp$ conservation rules.[12] In large devices, the heavy-hole (HH) and light-hole (LH) branches of the dispersion each give rise to a single subband for our well width: the $I(V)$ characteristic at $T=1.7$ K of a large $D=2$ μm device are shown in Fig. 1. The agreement between measured and predicted resonant peak positions is excellent,[10] so the peak positions provide experimental access to the energies of the quantized states in the strained SiGe well.

Moreover, since the strain in the well contributes to the energy separation HH–LH,[1,13] tunneling spectroscopy provides direct access to the magnitude of the biaxial strain. When a mesa is etched through the strained SiGe regions, the strain can relax by lateral displacement of the free surface.

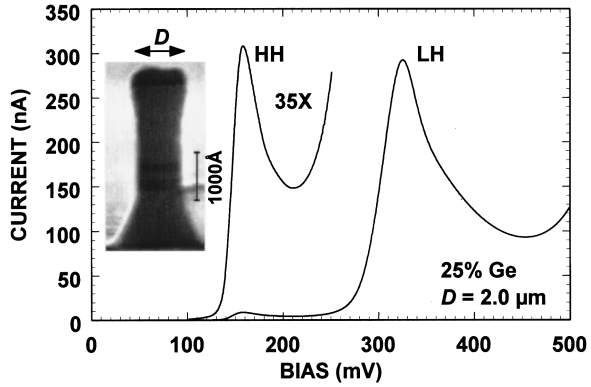

FIG. 1. $I(V)$ characteristics of a large $D=2$ μm $Si/Si_{0.75}Ge_{0.25}$ device at $T=1.7$ K, showing the peaks corresponding to resonant tunneling through the HH and LH subbands. Expanded $\times$35 view of the HH $I(V)$ peak is also shown. Inset shows the scanning electron micrograph of a representative mesa with nominal diameter $D=0.15$ μm prior to planarization.

[a)]Electronic mail: akyuz@brown.edu

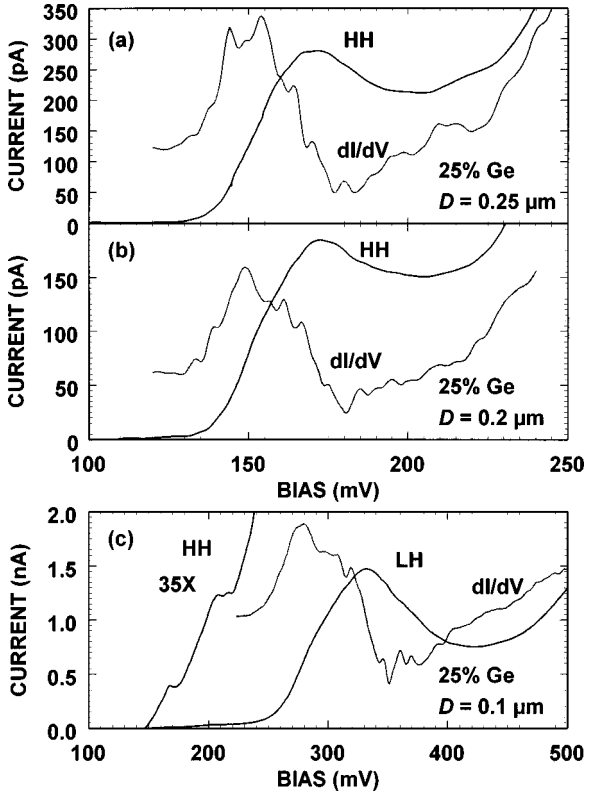

FIG. 2. $I(V)$ and dI/dV characteristics of smaller $Si/Si_{0.75}Ge_{0.25}$ structures with $D \leqslant 0.25$ μm at $T=1.7$ K. The HH $I(V)$ peaks of $D=0.25$ μm (a) and $D=0.2$ μm (b) structures exhibit clear and reproducible quasiperiodic fine structures, while the LH peaks for these D remain smooth. When $D=0.1$ μm (c), the HH peak changes qualitatively into two well-resolved steps, while the LH peak begins to exhibit a fine structure.

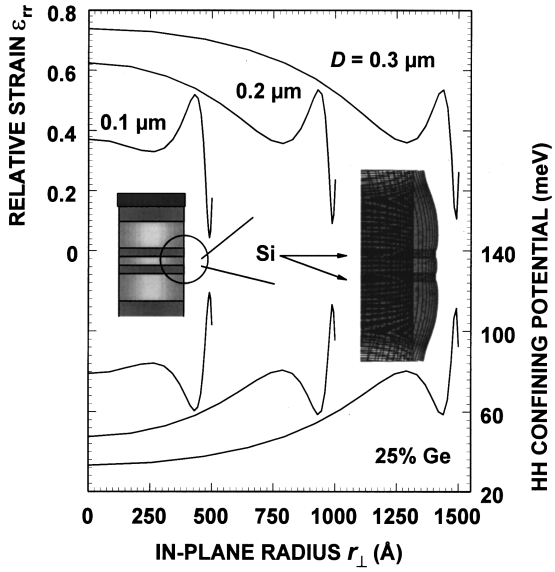

FIG. 3. The top curves show the calculated radial strain component ε_{rr} as a function of radius $r_\perp$ for $D=0.1$, 0.2, and 0.3 μm devices on the midplane of the SiGe well (full biaxial strain corresponds to $\varepsilon_{rr}=1$). Inset shows the magnified displacement of the finite element mesh corresponding to a section of the active region near the sidewall. The bottom curves are the corresponding in-plane confining potentials for the heavy-hole states as function of $r_\perp$. Note that in the $D=0.1$ μm case, the ground state is effectively confined to narrow ringlike region at the perimeter.

Previously, we reported a consistent shift of the HH and LH resonant peaks closer together as D decreased in the $0.25 \leqslant D < 1$ μm range, reflecting sizeable average strain relaxation.[11] Here we present data on deep-submicron structures in the $D \leqslant 0.25$ μm range which exhibit fine structure in the resonant peaks that provide experimental information on inhomogeneous strain in these quantum dots.

The HH resonant peaks of $D=0.25$ and 0.2 μm structures are shown in Figs. 2(a) and 2(b), respectively. These peaks exhibit a quasiperiodic fine structure, particularly clear in the dI/dV, with a separation between features of ~ 7 mV corresponding to an energy separation of ~ 2 meV. For these values of D, the LH peak line shape does not change from the large device $I(V)$ of Fig. 1, apart from the shift in peak position due to average strain relaxation.[11] The lack of observable fine structure in the LH peaks is consistent with the heavier in-plane mass predicted for light holes in a quantum well.[2] Figure 2(c) shows both the HH and LH $I(V)$ peaks of a $D=0.1$ μm device. Here the HH peak has changed qualitatively into a step-like structure on a rising current background. The step separation is ~ 35 mV (~ 8 meV) and the higher step is split into two closely spaced features. The LH resonant peak at $D=0.1$ μm has developed a fine structure quite similar to that exhibited by HH peaks in larger devices. The fine structure is consistent in the $I(V)$ of both polarities and reproducible upon temperature cycling. The current densities scale with nominal device diameter. For all devices, the geometric lateral quantization energy scale $\hbar^2/2m^*D^2$ and the single-carrier charging energy e^2/C are much smaller than the fine structure period.[14]

We attribute the resonant peak fine structure to lateral quantization in potentials due to inhomogeneous strain. Lateral displacement of the strained SiGe creates strain gradients as a function of the radial coordinate $r_\perp$. We have calculated the strain components by a finite element simulation based on a linear elastic model:[15] a cylindrical pillar of diameter D with SiGe layers fully strained to the silicon substrate is allowed to relax to a state of minimum energy. The geometry of the calculation is illustrated in the inset of Fig. 3, where the lateral displacement of the free surface of the pillar is magnified for clarity. The dominant effect is the relaxation of the in-plane strain component ε_{rr}, which is plotted as a function of $r_\perp$ on the midplane of the SiGe well for various D in Fig. 3 (top curves). Strain relaxation becomes a greater effect as D decreases, as expected. However, the behavior of $\varepsilon_{rr}(r_\perp)$ is nontrivial: while the radial strain decreases gradually with $r_\perp$ from the center of the pillar ($r_\perp \equiv 0$), the calculation predicts a region of increasing strain near the surface. The result is a ringlike region with $\varepsilon_{rr} \approx 0.5$ and a radial extent of ~ 100 Å running around the perimeter of the structure for all D.

We estimate the in-plane confining potential for heavy-hole states by retaining only the ε_{rr} component that is most affected by strain relaxation. We then calculate the HH subband energy at $k_\perp = 0$ as a function of local strain $\varepsilon_{rr}(r_\perp)$ by the usual six-band Luttinger–Kohn Hamiltonian.[2] The resulting lateral potentials for heavy-hole states are shown on the bottom of Fig. 3. The regions with larger ε_{rr} are local potential minima for HH states. Accordingly, as shown in Fig. 3, the lateral confining potential for $D \geqslant 0.2$ μm structures looks like a two-dimensional parabola with a weak ringlike

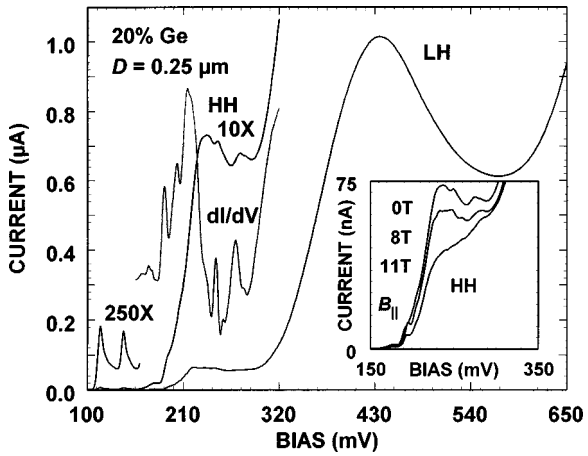

FIG. 4. $I(V)$ characteristics of a $D=0.25\ \mu$m structure from a different wafer with a $Si/Si_{0.8}Ge_{0.2}$ design at $T=1.7$ K, showing strong heavy-hole lateral quantization. Inset shows the quenching of the fine structure in the HH peak by a parallel ($\mathbf{B}\|\mathbf{I}$) magnetic field.

perturbation near the sidewall, while for the smaller $D=0.1\ \mu$m structure it is the ring that confines the ground state. The effective height of the lateral confinement is ~ 15 meV. It should be emphasized that analogous strain gradients appear in the SiGe emitter region (see inset of Fig. 3), but there, the lateral potential is screened by the large density of holes. Consequently, the observed fine structure arises principally from the lateral quantization in the well, where the density of dynamically stored holes is much smaller than in the emitter.[14] Given the confining HH potentials of Fig. 3, one can estimate the lateral confinement energies using interpolated HH effective mass at $k_\perp=0$. The result is that for the $D=0.2\ \mu$m structure, the lowest-lying states are confined near $r_\perp=0$ by the approximately parabolic potential and separated by ~ 2 meV. Conversely, in the $D=0.1\ \mu$m device, the two lowest-lying states are confined to a narrow ring at the perimeter and their energy separation is on the order of ~ 10 meV. These estimates of lateral energy quantization are in excellent agreement with the observed HH peak line shapes, which evolve from relatively weak quasiperiodic fine structure at $D=0.25\ \mu$m to two well-resolved current steps at $D=0.1\ \mu$m (consistent with the sharp outer ring potential).

In order to confirm our findings, we have fabricated dots from another $Si_{1-x}Ge_x$ RT wafer with similar well and barrier specifications as the $x=0.25$ structure of Figs. 1 and 2, but with $x=0.2$ Ge content and larger SiGe emitter and collector reservoirs. The decrease in x reduces the Si/SiGe valence band discontinuity, leading to larger tunneling current density and better resolution of the fine structure, as shown for a $D=0.25\ \mu$m device in Fig. 4. Because of the larger undoped SiGe regions outside the double barrier, the resonant peaks in the $I(V)$ appear at higher bias. As previously, the LH peak for this D remains smooth while the HH peak exhibits a strong fine structure with a quasiperiod ~ 15 mV (~ 2.5 meV). In addition, two sharp subthreshold peaks appear at low bias, separated by ~ 27 mV, which corresponds to ~ 4.5 meV of energy level separation. The origin of these subthreshold peaks, which survive temperature cycling, is still under study. The structure of the HH peak, however, is consistent with inhomogeneous-strain-induced lateral confinement in a potential similar to Fig. 3. The magnetotunneling $I(V,B_\|)$ data on this same HH peak are shown in the inset of Fig. 4. As $B_\|$ is parallel to the tunneling direction, the $B_\|$-induced confinement is superimposed on the lateral strain-induced potential. The structure in the HH peak is quenched near $B_\|=9$ T. This implies that the strain-induced lateral potential length scale confining the HH states is comparable to the ~ 100 Å magnetic length at 9 T, again is consistent with the calculated potentials in Fig. 3.

In conclusion, we have used resonant tunneling measurements to probe the inhomogeneous strains and associated potentials in individual p-$Si/Si_{1-x}Ge_x$ double-barrier resonant tunneling structures of diameter D in the $0.1<D\leqslant 0.25\ \mu$m range. In the tunneling current we observed fine resonances through strain-induced quantum dot states that became stronger in devices with smaller D. We correlated the measured heavy-hole fine structure with the confining potentials corresponding to the nonuniform strain distributions predicted by finite element analysis. Interestingly, strain gradients near the radius of our devices create a ring-like confining potential at the perimeter which confines the ground state in sufficiently small $D\leqslant 0.15\ \mu$m structures. Our measurements prove tunneling to be a useful spectroscopic probe for strain phenomena in individual nanostructures, and point out the surprisingly large influence inhomogeneous strain will exert on the electronic properties of proposed nanodevices.

The authors thank H. Johnson for useful discussions and A. Schwartzman for microscopy assistance. This work has been supported in part by an NSF Career Award (DMR-9702725), the ONR Young Investigator Program (N00014-95-l-0729), and a Sloan Foundation Fellowship.

[1] G. L. Bir and G. E. Pikus, *Symmetry and Strain-Induced Effects in Semiconductors* (Wiley, New York, 1974).
[2] J. M. Luttinger and W. Kohn, Phys. Rev. **97**, 869 (1955); J. M. Luttinger, Phys. Rev. **102**, 1030 (1956).
[3] C. G. Van de Walle and R. M. Martin, Phys. Rev. B **34**, 5621 (1986).
[4] K. Kash, B. P. Van der Gaag, D. D. Mahoney, A. S. Gozdz, L. T. Florez, and J. P. Harbison, Phys. Rev. Lett. **67**, 1326 (1991).
[5] D. Gershoni, rJ. S. Weiner, S. N. G. Chu, G. A. Baraff, J. M. Vandenberg, L. N. Pfeiffer, K. West, R. A. Logan, and T. Tangun-Ek, Phys. Rev. Lett. **65**, 1631 (1990).
[6] T. Arakawa, S. Tsukamoto, Y. Nagamune, M. Nishioka, J. H. Lee, and Y. Arakawa, Jpn. J. Appl. Phys., Part 1 **32**, 1377 (1993).
[7] D. Leonard, M. Srishnamurthy, C. M. Reaves, S. P. Denbaars, and P. M. Petroff, Appl. Phys. Lett. **63**, 3203 (1993).
[8] J. M. Moison, F. Houzay, F. Barthe, L. Leprince, E. André, and O. Vatel, Appl. Phys. Lett. **64**, 196 (1994).
[9] N. N. Ledentsov, D. Bimberg, Yu. M. Shernyakov, V. Kochnev, M. V. Maximov, A. V. Sakharov, I. L. Krestnikov, A. Yu. Egorov, A. E. Zhukov, A. F. Tsatsul'nikov, B. V. Volovik, V. M. Ustinov, P. S. Kop'ev, Zh. I. Alferov, A. O. Kosogov, and P. Werner, Appl. Phys. Lett. **70**, 2888 (1997).
[10] A. Zaslavsky, D. A. Grützmacher, S. Y. Lin, T. P. Smith III, R. A. Kiehl, and T. O. Sedgwick, Phys. Rev. B **67**, 16036 (1993).
[11] A. Zaslavsky, K. R. Milkove, Y. H. Lee, B. Ferland, and T. O. Sedgwick, Appl. Phys. Lett. **67**, 3921 (1995).
[12] S. Luryi, Appl. Phys. Lett. **47**, 490 (1985).
[13] R. People, Phys. Rev. B **32**, 1405 (1985).
[14] V. J. Goldman, D. C. Tsui, and J. E. Cunningham, Phys. Rev. B **35**, 9387 (1987).
[15] These calculations were performed using the ABAQUS finite element code for mechanical analysis (Hibbitt, Karisson & Sorensen, Inc., Pawtucket, RI).